24-040

Explosion-Proof Enclosure Failure to Contain a Lithium-Ion Battery Thermal Runaway

Thomas H. Dubaniewicz
CDC NIOSH, Pittsburgh PA

ABSTRACT

Gassy underground mines commonly use explosion-proof (XP) enclosures to enclose electrical ignition sources to prevent propagation of an internal methane-air explosion to a surrounding explosive atmosphere. Researchers at the National Institute for Occupational Safety and Health (NIOSH) conducted a lithium-ion battery thermal runaway test within a modified MSHA-approved XP enclosure to assess thermal runaway containment. Thermal runaway produced jet flames emanating from the cover joint at several locations and distorted the cover joint and bottom plate of the enclosure beyond allowable limits. The test demonstrates that XP enclosures may not provide adequate explosion protection against lithium-ion battery thermal runaway. This paper suggests some approaches to mitigate the hazard.

INTRODUCTION

Lithium-ion (Li-ion) battery fires are becoming more commonplace in the United States. Fire departments across the country held a week-long safety stand-down during June 2023 themed "Lithium-Ion Batteries: Are You Ready?" [1]. Large-format Li-ion powered battery electric vehicles (BEVs) are in the early stages of deployment in underground mines in the United States. GlobalData [2] reported a total of 10 active electric Load Haul Dump (LHD) vehicles and trucks in U.S. underground mines as of March 2022. A Li-ion BEV fire at an underground operation in Nevada prompted a U.S. Mine Safety and Health Administration (MSHA) order to suspend operations to protect the mine workers at the operation [3]. The Nevada incident represents a failure rate of well into the percent range for fires per deployed Li-ion battery LHDs and trucks in U.S. underground mines. Several Li-ion battery truck fires have occurred in Canadian underground mines as well [4, 5], representing a failure rate in the percent range for a larger sample size of 76 electric LHDs and trucks [2]. All of these incidents involved heating from short circuits external to the battery or external to multiple cells within a large battery rather than a single-cell internal short circuit.

Li-ion BEVs in gassy underground mines pose unique explosion hazards. Dubaniewicz et al. [6, 7] reviewed the gassy mine explosion hazard and the use of explosion-proof (XP) or flame-proof enclosures for explosion protection of electrical equipment. Mines commonly use XP or flame-proof enclosures in potentially explosive atmospheres to enclose electrical ignition sources to prevent propagation of an internal methane-air explosion to a surrounding methane and coal-dust-contaminated atmosphere. Emergencies involving ventilation disruption may produce explosive atmospheres. Stranded battery energy is one potential ignition hazard after mine power is shut off during such

emergencies [8]. Mine rescue robots and drones offer the potential to provide supply, surveillance, and sensing capabilities that are critical for search and rescue operations. Ali [9] identified several attempts to develop mine rescue robots. Ali indicated that several rescue robots are currently being developed, and a few have been tested in real-world circumstances, albeit with unsatisfactory outcomes. Ali asserted that the challenge for the industry is to make more advanced, smarter rescue robots with strong and reliable hardware to work in dangerous zones.

Dubaniewicz et al. [10] reported that Li-ion battery thermal runaway may produce excessive pressures within sealed enclosures that provide relatively little free space around the battery. Results of that work support consideration for revision of safety standards, such as the IEC 60079-1 edition 8 Equipment protection by flameproof enclosures "d", because the standard does not provide assessment criteria for Li-ion battery thermal runaway failure modes. The work also suggests that, where battery enclosure internal volume restrictions may prevent adequate free space, thermal runaway cascade prevention and venting with properly designed and maintained flame arrestors are potential mitigation strategies for excessive overpressures.

XP enclosures typically include a cover with a flame quenching joint, cable entrance, and may include an auxiliary pressure-relief device. The maximum internal pressure during the ignition of an explosive air mixture in an enclosure is directly related to the amount of venting through flame quenching gaps and auxiliary pressure-relief devices [11]. This raises the question as to whether the flame quenching gaps of conventional XP enclosures provide sufficient pressure relief and quench a Li-ion battery thermal runaway, without the need for an auxiliary pressure-relief device. In this work, researchers at the National Institute for Occupational Safety and Health (NIOSH), Pittsburgh Mining Research Division (PMRD), initiated a Li-ion battery thermal runaway within a modified commercial XP enclosure to see if venting through the cover joint and leakage through the cable entrance provided sufficient pressure relief while preventing excessively hot gasses from escaping.

MATERIALS AND METHODS

Figures 1, 2, and 3 show the battery pack and XP enclosure. The battery pack consisted of thirty-nine model MH1 Nickel Manganese Cobalt (NMC) 811 18650 cells arranged in a 13 series by 3 parallel configuration. The MH1 cell ratings were 3.2 Ah, 3.67 V, and 11.7 Wh. A multichannel potentiostat/galvanostat (MSTAT, Arbin Instruments, College Station, Texas) cycled the cells using cell-manufacturer-specified parameters. The cells were conditioned with

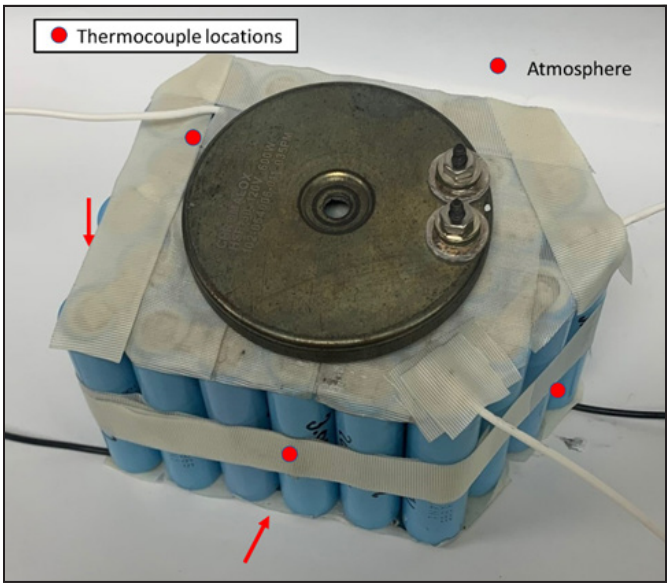

Figure 1. Battery pack with disk heater on top. Arrows point towards thermocouple locations out of view

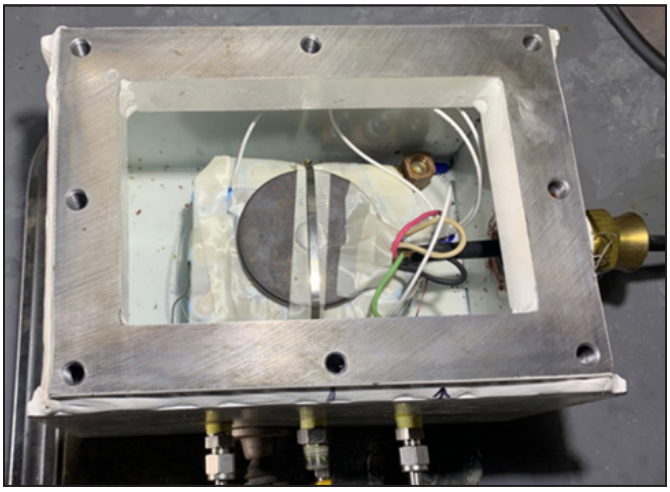

Figure 2. Battery pack placed within XP enclosure

three charge-discharge cycles followed by a charge to 100% state of charge. The battery voltage at the start of the test was 53.7 V. Table 1 lists the battery electrical parameters. A 240 W disk heater was placed on top of the battery pack to initiate thermal runaway. The disk heater contacted multiple cells to simulate heating such as from external short circuits. Disk heater activation marked the start of the test.

The XP enclosure's specified dimensions were approximately 10.375 inches (16.4 cm) in length by 7.375 inches (18.7 cm) in width by 6.156 inches (15.6 cm) in depth (less cover). The enclosure was made from welded steel with a 0.507-inch (1.29-cm) thick flat aluminum cover bolted to the enclosure. The enclosure walls were approximately

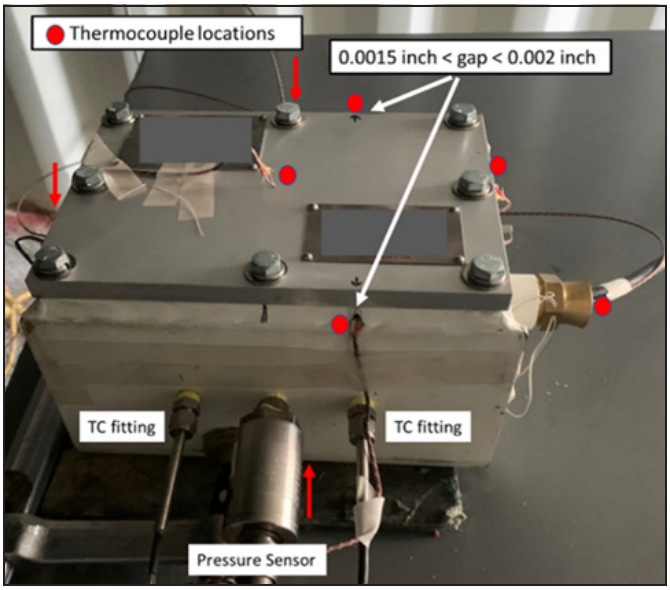

Figure 3. XP enclosure with bolted cover. Locations of the largest flame-arresting gaps and placement of thermocouples and fittings shown. Arrows point towards thermocouple locations out of view

Table 1. Battery electrical parameters

	Voltage	Capacity (Ah)	Energy (Wh)
Rated	47.7	9.6	458
Measured	53.7	9	429

0.25 inches (0.635 cm) thick. The cover flange flame path was approximately 1.125 inches (2.86 cm) in length. A 5,550-ml (339 cubic inches) internal volume was measured by filling it with water. With the battery and disk heater placed inside, the free space within the enclosure was estimated to be 4,870 ml. The free space-to-battery volume ratio was estimated to be 7.54. Researchers bolted the cover in place per manufacturer's instructions and probed the cover joint flame gaps with feeler gauges. A 0.0015-inch (0.038-mm) feeler gauge penetrated the cover joint at two locations shown in Figure 3. A 0.002-inch (0.051-mm) feeler gauge was unable to penetrate the cover joint anywhere, indicating that the plane joint clearances were within allowable limits (<0.004 inch (0.1 mm)) per U.S. Code of Federal Regulations [12]. Researchers fed a 4-conductor type P cable through a stuffing box cable entrance and used it to monitor battery voltage and to power the disk heater. The cable was secured in the cable entrance per manufacturer's instructions. Researchers modified the enclosure by drilling and tapping three 7/16-inch holes for national pipe taper (NPT) fittings to route thermocouples into the enclosure and to connect a 3,000-psi (207-bar) pressure sensor to the enclosure's side wall. These modifications invalidate the MSHA approval. Researchers selected the pressure sensor range based on pressures measured for a comparable free space-to-battery volume ratio [10]. Pressures were sampled at 100 samples per second.

Thermocouples (TCs) were placed at various locations on the battery and external enclosure surfaces and joints (Figures 1 and 3). The TCs placed within the enclosure were sheathed type N (0.81-mm diameter). These sheathed TCs were epoxied within a steel tube fitting through the enclosure wall to maintain an air-tight seal. Unsheathed type K TCs were used on external surfaces and joints. Temperatures were sampled at 10 samples per second.

The thermal runaway test was conducted in a container with dimensions of 12-m long, 2.4-m wide, and 2.85-m high (40 ft × 8 ft × 9.5 ft) (Figure 4) [13]. A fan installed at one end of the container provided 0.2 m/s of ventilation velocity. Gas samples were drawn by sampling tubes to an infrared gas analyzer to measure carbon monoxide and carbon dioxide concentrations. The sampling tubes were located a few meters downwind from the XP enclosure. Gas measurements were sampled at 10 samples per second. Video and thermal imaging cameras recorded the thermal runaway test.

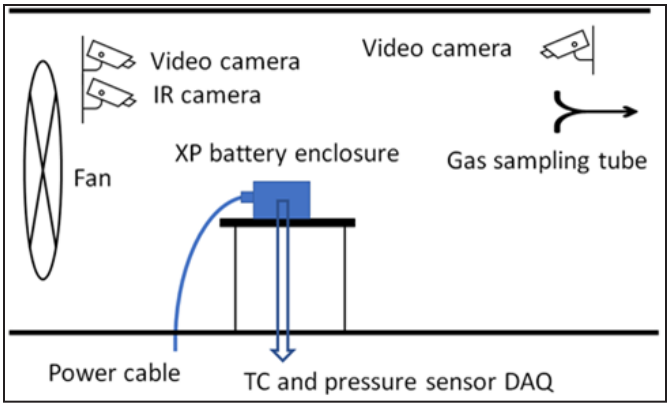

Figure 4. Drawing of battery thermal runaway test setup with fan, cameras, and instrumentation connections

RESULTS AND DISCUSSION

The disk heater initiated a cascading battery thermal runaway approximately 49.5 minutes into the test. Jet flames emanating from the cover joint at several locations could be discerned through thick smoke (Figure 5). The jet flames appeared to be blue near the joint. Discharge of flame is a failure criterion per U.S. Code of Federal Regulations [12]. The thermal imaging camera revealed hot gasses extending well beyond the cover joint through the smoke. Joint and cable entrance peak temperatures were 1,097 and 138 °C,

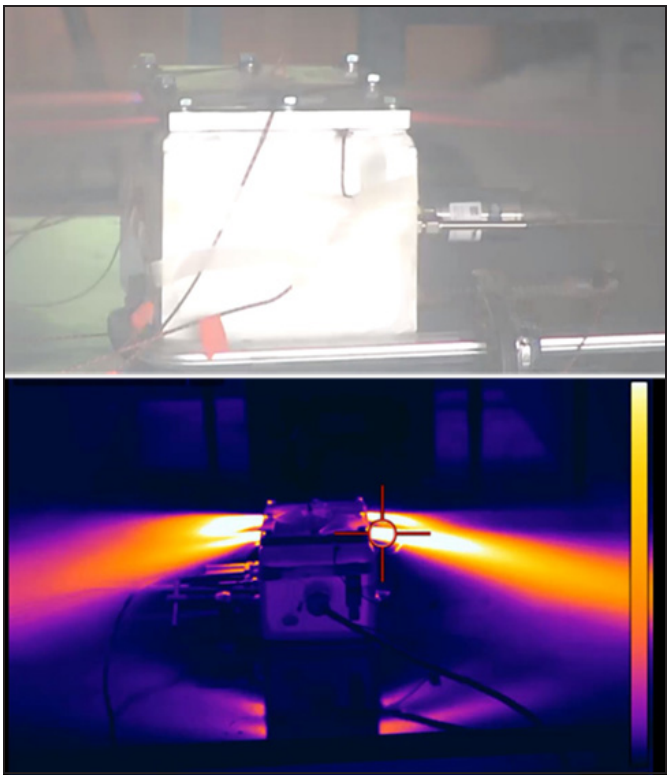

Figure 5. Video and infrared camera images of jet flames emanating from cover joint

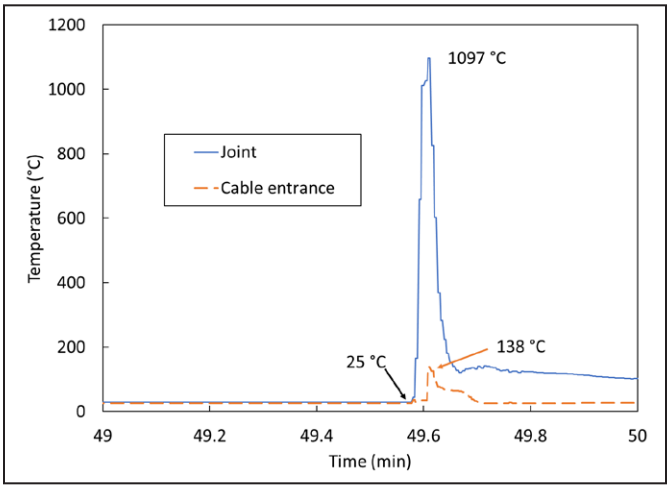

Figure 6. Time traces of cover joint and cable entrance temperatures external to the XP enclosure

respectively, and both were 25 °C at the thermal runaway onset (Figure 6). No flame was observed from the cable entrance.

The thermal runaway cascade proceeded rapidly throughout the battery as indicated by temperature measurements at several battery locations (Figure 7). A post-test

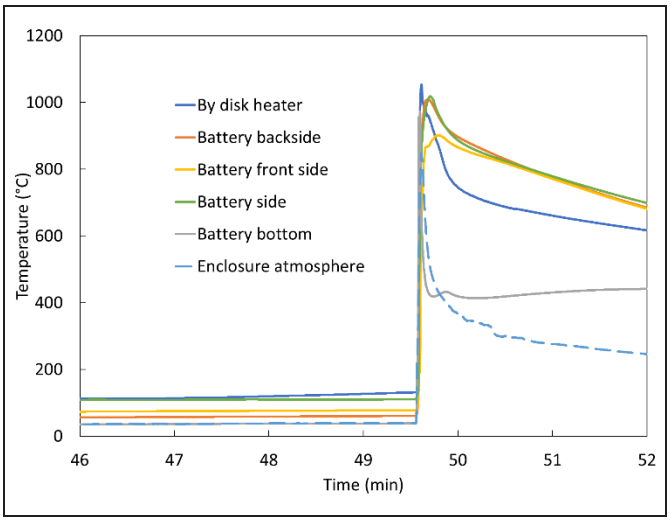

Figure 7. Time traces of battery pack and atmospheric temperatures inside of the XP enclosure

Table 2. Temperatures measured inside of the XP enclosure.

Thermocouple Location	At Thermal Runaway Onset (°C)	Peak (°C)
By disk heater	130	1054
Battery backside	61	1009
Battery front side	79	901
Battery side	111	1018
Battery bottom	39	974
Enclosure atmosphere	39	849

inspection confirmed that thermal runaway occurred in all of the cells. Table 2 lists battery and enclosure internal atmosphere temperatures just before and at the peak of thermal runaway. A higher temperature of 1097 °C was measured outside of the enclosure (Figure 6). The 1097 °C measurement is also higher than MH1 cell thermal runaway temperatures measured within sealed enclosures [10]. Yuan et al. [14] found that the MH1 cell (identified as NMC 2) thermal runaway produced significant amounts of inert carbon dioxide gas and flammable gasses including hydrogen, carbon monoxide, methane, and lesser amounts of a few heavier hydrocarbons. MH1 cell thermal runaway produces about 0.66 liters of gas per watt hour of battery energy [10], corresponding to 283 liters of gas generated by the 429 Wh battery pack. Gas generation from the battery should displace atmospheric oxygen from the XP enclosure to an extent. Even with the generation of inert carbon dioxide and apparent displacement of atmospheric oxygen internally, the flammable gasses evidently mixed with sufficient amounts of atmospheric oxygen outside of the enclosure and were ignited by the hot gasses escaping the joint to produce a higher temperature externally.

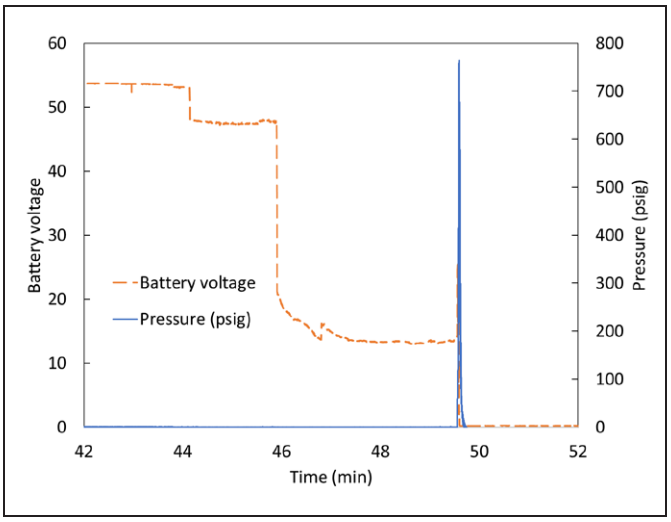

Figure 8. Battery voltage dropped several minutes before thermal runaway pressure spiked

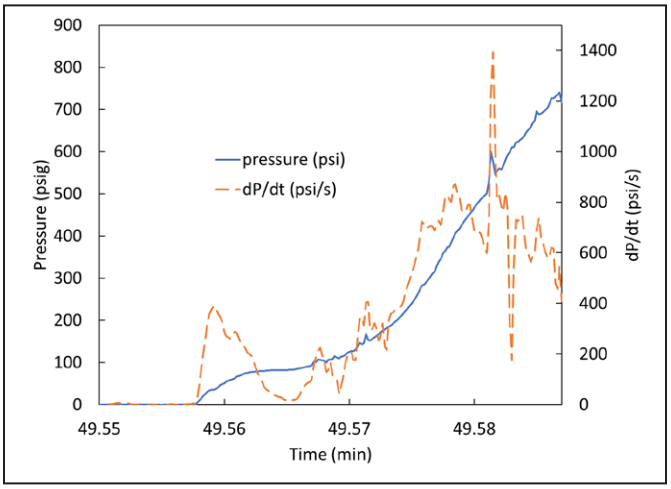

Figure 9. Time traces of pressure and time rate of pressure during thermal runaway

An abrupt pressure rise occurred at thermal runaway preceded by a drop in battery voltage (Figure 8). The voltage drop prior to thermal runaway indicates battery shorting. Figure 9 shows an expanded view of the pressure and pressure time rate (dP/dt) during thermal runaway. An apparent 60 Hz interfering signal (40 Hz perceived frequency at 100 samples per second) became more prominent as thermal runaway progressed. The interfering signal is most prominent in the dP/dt time trace. It is thought that the interfering signal originated at the disk heater power leads and was conducted to the metallic enclosure wall in electrical contact with the pressure sensor body. Taking the interfering signal into consideration, the peak pressure and pressure rising rate are estimated to be in excess of 700 psig (48.3 barg) and 800 psi/s (55.2 bar/s), respectively.

Figure 10. A 0.004-inch feeler gauge penetrated the cover joint in several places after the thermal runaway test

The thermal runaway pressure distorted the enclosure beyond allowable limits. Researchers checked joint clearances with a feeler gauge after the test, and several gaps were found in excess of 0.004 inch (0.1 mm) (Figure 10), which does not conform with U.S. Code of Federal Regulations [12]. Escaping gasses etched a path through soot that accumulated in the cover joint as shown in Figure 11. Thermal runaway deformed the XP enclosure bottom plate about 4 mm (0.16 inch) over the 18.7-cm (7.36-inch) dimension (Figure 12), exceeding the 0.040 inch per lineal foot of permanent distortion permitted by U.S. Code of Federal Regulations [12].

Figure 13 shows the effect of MH1 battery gas leakage from the XP enclosure by comparison to sealed enclosures in terms of thermal runaway pressures and dP/dt. The MH1 cell data for the sealed enclosures is from Dubaniewicz et al. [10]. The sealed enclosure data was obtained under near-adiabatic conditions that impeded heat loss through the enclosure walls. The gas leakage from the XP enclosure and heat sinking to the enclosure walls reduced the pressure and pressure rise rate to a great extent, but not nearly enough to prevent excessive distortions to the cover joint and bottom wall.

The battery thermal runaway generated high levels of carbon monoxide (1,440 ppm) and carbon dioxide (989 ppm) as sampled several meters downwind from the battery (Figure 14). Besides being toxic, carbon monoxide-air mixtures are flammable between 12% and 75% by volume

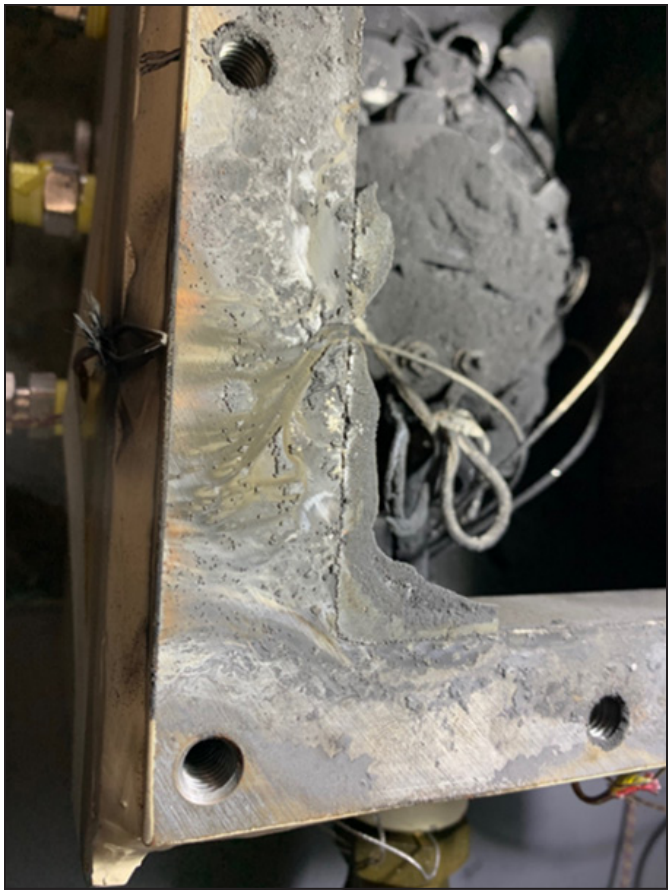

Figure 11. Escaping gasses etched a path through soot that accumulated in the cover joint

Figure 12. Thermal runaway pressure deformed the XP enclosure bottom plate beyond allowable limits

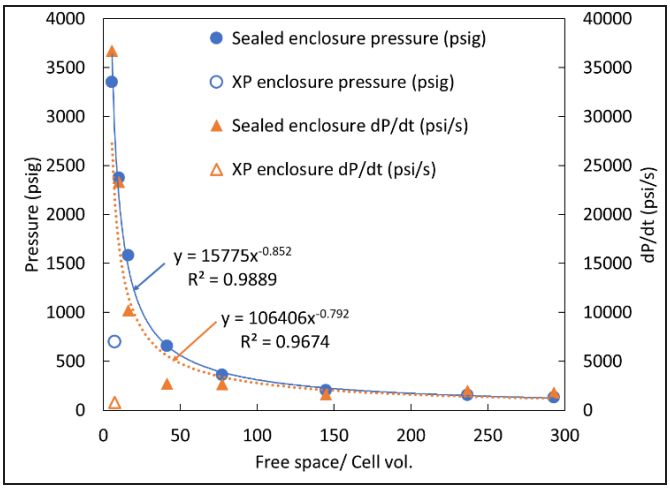

Figure 13. XP enclosure pressure and pressure rise rate compared to sealed enclosure pressures and pressure rise rates

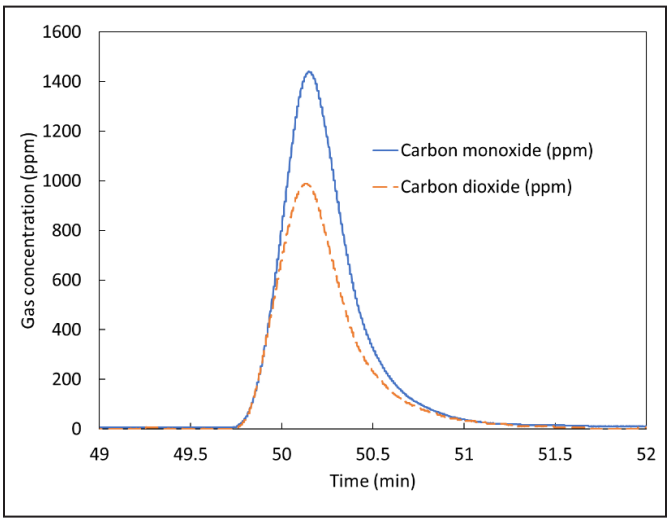

Figure 14. Time traces of carbon monoxide and carbon dioxide sampled several meters downwind from the battery thermal runaway

with air. Carbon dioxide is inert and displaces other gasses to impede combustion.

Where battery enclosure internal volume restrictions may prevent adequate free space, thermal runaway cascade prevention and venting with properly designed and maintained flame arrestors are potential mitigation strategies for excessive overpressures [10]. Limiting thermal runaway to a small portion of a battery can reduce the amount of gas-generated pressure. Properly designed and maintained flame arrestors may provide pressure relief of ignitions within sealed enclosures while preventing ignition of a surrounding

explosive atmosphere. For example, NIOSH has contracted with various organizations to evaluate thermal runaway, ascertain methods for preventing and controlling thermal runaway, and develop specific controls such as flame arrestors and debris containment systems for thermal runaway containment [15, 16, 17]. These contracts were developed to complement the current research NIOSH conducts internally on Li-Ion battery safety. In particular, NIOSH contracted with ADA Technologies, Inc. to develop a flame arrestor and debris containment system for quenching Li-ion battery thermal runaway [15]. A small-scale prototype system was built and tested successfully. This system is currently going through their commercialization process to be available to the mining industry. However, the evaluation of this or other flame arrestor and debris containment systems is outside the scope of this experiment and follow-on research on the efficacy of auxiliary flame arrestors for Li-ion battery enclosures is warranted.

LIMITATIONS

The findings and conclusions from this study are based on a limited sample set investigated under specific conditions. Specifically, a commercially available XP enclosure was selected based on the battery pack dimensions, free space considerations, and facility capabilities for full scale testing to enable the monitoring and evaluation of the thermal runaway event. The enclosure was also modified to install temperature and pressure sensors which may have impacted the design specifications as deployed in underground mining environments. Other XP enclosures may have different constructions and may produce different results than reported here. Other Li-ion battery chemistries, cell configurations, and capacities may have different thermal runaway characteristics and may produce different results than reported here. Other thermal runaway initiation methods may produce different results than reported here.

CONCLUSION

The potential for excessive pressures, temperatures, and flammable gasses generated by Li-ion battery thermal runaway should be taken into consideration if planning to use conventional XP enclosures as battery enclosures in gassy underground mines.

DISCLAIMER

The findings and conclusions in this report are those of the authors and do not necessarily represent the official position of the National Institute for Occupational Safety and Health, Centers for Disease Control and Prevention. Mention of any company or product does not constitute endorsement by NIOSH.

ACKNOWLEDGMENT

The author thanks Richard Thomas and John Soles of the Pittsburgh Mining Research Division for setting up and conducting the thermal runaway test.

REFERENCES

[1] Safety Stand Down (2023). Lithium-Ion Batteries: Are You Ready? Safety Stand Down. Retrieved August 2023 from www.safetystanddown.org.

[2] GlobalData (2022). Electric Vehicles in Surface and Underground Mining. GlobalData Plc, London UK.

[3] Stewart D (2022). Nevada Gold Mines BEV Adoption Plan and Safety Concerns. Presentation at the BEV Fire Safety Workshop, Missouri S&T, June 2022.

[4] Gillett S (2021). Battery Electric Vehicle Emergency Response Incident Review and Best Practices. Workplace Safety North Virtual Symposium: Battery Electric Vehicle Safety in Mines, January 20, 2021. Retrieved August 2023 from www.workplacesafetynorth.ca/resources/virtual-symposium-battery-electric-vehicle-safetymines.

[5] Jacques D (2019). BEV Pioneering Partnership at Borden—Celebrate the Wins, Face the Challenges. Mining Diesel Emissions Council. MDEC 2019, October 7-10, Toronto, ON. S6P3. Retrieved August 2023 from mdec.ca/2019/S6P3_David_Jacques.pdf

[6] Dubaniewicz TH, DuCarme JP (2016). Internal short circuit and accelerated rate calorimetry tests of lithium-ion cells: considerations for methane-air intrinsic safety and explosion proof/flameproof protection methods. J Loss Prev Process Ind 43:575–584. Retrieved August 2023 from www.ncbi.nlm.nih.gov/pmc/articles/PMC5040472/.

[7] Dubaniewicz TH, Zlochower I, Barone T, Thomas R, Yuan L, (2021). Thermal runaway pressures of iron phosphate lithium-ion cells as a function of free space within sealed enclosures. Mining, Metallurgy & Exploration 38, 539–547. doi.org/10.1007/s42461-020-00349-9.

[8] Dubaniewicz TH (2009). From Scotia to Brookwood, fatal US underground coal mine explosions ignited in intake air courses. J. Loss. Prev. Proc. Ind. 22(1) 2009. 52-58.

[9] Ali O (2022). How are robots used in mine rescue operations? AZO Mining. June 30, 2022. www.azomining.com/Article.aspx?ArticleID=1698.

[10] Dubaniewicz TH, Barone TL, Brown CB, Thomas RA (2022). Comparison of thermal runaway pressures within sealed enclosures for nickel manganese cobalt and iron phosphate cathode lithium-ion cells. Journal of Loss Prevention in the Process Industries 76:104739.

[11] Morley LA (1990). Mine Power Systems. U.S. Department of the Interior, Bureau of Mines. Information Circular 9258.

[12] U.S. Code of Federal Regulations (2023). Title 30, Part 18, Section 18.31 Enclosures—joints and fastenings; Title 30, Part 18, Section 18.62. Tests to determine explosion-proof characteristics. Retrieved August 2023 from www.ecfr.gov/current/title-30/chapter-I/subchapter-B/part-18.

[13] Yuan L, Tang W, Thomas R, Soles J (2023). Evaluation of different suppression techniques for lithium-ion battery fires. Proceedings of the 19th North American Mine Ventilation Symposium, Edited by Purushotham Tukkaraja, pp. 384-392, CRC Press, ISBN 978-1-032-55146-3.

[14] Yuan L, Dubaniewicz T, Zlochower I, Thomas R, Rayyan N (2020). Experimental study on thermal runaway and vented gases of lithium-ion cells. Process Safety and Environmental Protection 144:186-192.

[15] Gunter B, Kamboj S (2023). High Energy Battery Thermal Runaway Alleviation Protection (TRAP) Flame Arrestor for Mine Safety. NIOSH Contract No. 75D301-21-C-11477.

[16] Roth, K. and Gunter, W. (2021) Multi-cell Lithium Ion Battery Safety Enhancement for Underground Mining Applications via Cell-to-Cell Isolation During Thermal Runaway. NIOSH Contract No. 75D301-19-C-05904.

[17] Jones K, Bhattacharya S, and Surampudi B (2021). Safety Enhancing Technologies for Usage of Multi-Cell Battery Power Systems in Underground Equipment. NIOSH Contract No. 75D301-19-C-05506

24-041

Fleet Efficiency Evaluations for Optimal Cycle Times Through Various Blast Designs in the Sorted Geological Formation Under Constrained Operating Conditions

Venkata Aneesh, Kona
Pike Industries (A CRH Company), Belmont, NH

ABSTRACT

This paper examines the desired blast fragmentation results associated with mining fleet performance at Sidney Quarry of Pike Industries, A CRH Company by reducing cycle times and hauling less oversize material generated from the blast to the crusher to increase the overall plant throughput. We are constrained with blast patterns due to the poorly sorted and fractured seams in the quarry, which is angled at 35° NE and dipping at 80° and runs parallel to the Interstate-95 highway on the east of the quarry boundary about 600 ft, making it challenging to alter the blast patterns for optimal yield.

We evaluated multiple relationships between blast patterns in conjunction with loader diggability. Results analyzed include the digging hours, fleet cycle times, and the fragment size with the optimized blast design through 3GSM software to arrive at the optimal yield to maximize the crusher throughput.

Our primary objective is to focus on safety with efficient cycle times and clean floors & clean face generation for better operational efficiencies. Secondly, to optimize the crusher yield which is an integral part of quarry operation. Further, this paper provides the utilization of 3GSM blasting techniques in quarry applications with computer vision fragmentation analysis and VizaLogix, a fleet management software to analyze the cycle times sampling.

INTRODUCTION

The Sidney Plant, which produces ~650k tons/year (590k metric tonnes/year) supporting its vertically integrated asphalt plant for federal and state DOT projects, and local communities, is in Kennebec County, Maine, approximately 10 miles (18 kilometers) north of the state capital Augusta, and adjacent to the major east coast highway Interstate-95.

The stone is mined from the quarry by using conventional hammer drilling and non-electric blasting techniques and transported to the three staged crushing/grinding plants by a truck-loader mining fleet. A total of approximately 65k tons (59k metric tonnes) of waste material is mined each year at about a 0.1-unit waste to 1.0 unit of production rock. Quarry waste and overburden stripping ratios are expected to increase in the future and an optimal drill and blast program is very important to keep mining costs and productivity meeting the goals. A total of approximately 60 percent of the raw ingredients used in the Asphalt plant come from this quarry.

GEOLOGY

The rock type in the Sidney quarry is a Silurian rock of the Waterville Formation (Oshberg, 1968). The Quarry and the asphalt plant are mainly interested in mining gray pelite and quartzite wacke for aggregate production. In the future, the plan is to also mine the gray limestone (part of the formation) with 1-inch thick phyllite (Oshberg, 1968) interbedded in lower lifts on the west side of the quarry.

Skow is the name of the lowest lift and is currently under development. It gets its name from the contact line where the two stone units are mined together and named after a former Pike employee. The current pit consists of one bench with varied terrain, leaving the uneven bench height being 50–85 feet (15–25 meters).

The rock mass is extensively faulted and fractured. The fractures can be readily observed in the quarry highwalls.